Electrical transport, magnetism, and magnetoresistance in ferromagnetic oxides with mixed exchange interactions: A study of the $La_{0.7}Ca_{0.3}Mn_{1-x}Co_xO_3$ system

N. Gayathri,* A. K. Raychaudhuri,† and S. K. Tiwary
Department of Physics, Indian Institute of Science, Bangalore 560012, India

R. Gundakaram, Anthony Arulraj, and C. N. R. Rao
Solid State and Structural Chemistry Unit, Indian Institute of Science, Bangalore 560012, India

(Received 20 December 1996)

In this paper we report the results of an extensive investigation of the $La_{0.7}Ca_{0.3}Mn_{1-x}Co_xO_3$ system. Substitution of Mn by Co dilutes the double-exchange (DE) mechanism and changes the long range ferromagnetic order of $La_{0.7}Ca_{0.3}MnO_3$ to a cluster glass-type ferromagnetic (FM) order similar to that observed in $La_{0.7}Ca_{0.3}CoO_3$. This happens even for the lowest Co substitution of $x=0.05$ and persists over the entire composition range studied ($0.05 \leqslant x \leqslant 0.5$). The Co substitution also destroys the metallic state and the resistivity increases by orders of magnitude even with a very small extent of Co substitution. The charge localization due to Co substitution is likely to have its origin in polaronic lattice distortion. The Co substitution also suppresses the colossal magnetoresistance (CMR) of the pure manganate ($x=0$) over the entire temperature and composition range and it becomes very small for $x \geqslant 0.2$. We conclude that the DE interaction and the resulting metallic state is very ''fragile'' and hence even a small amount of Co substitution can destroy the FM order, the metallic state, and the CMR. [S0163-1829(97)00127-6]

I. INTRODUCTION

Transition metal oxides of the ABO_3 type display varieties of electronic transport and magnetic properties. Recently there has been renewed interest in physical properties of oxides with the general chemical formula $Ln_{1-x}A'_xMnO_3$ (Ln $=$La, Pr, Nd, etc., and $A'=$Ca, Sr, Ba, Pb, etc.) since these materials show some exotic electronic transport and magnetic properties and colossal magnetoresistance (CMR).[1–3] In these systems, the A sites of the ABO_3 structure are occupied by trivalent Ln or divalent A' ions leading to mixed valency of the transition metal ions (Mn^{3+}/Mn^{4+}) which occupy the B sites. In the particular context of the manganates the mixed valency leads to strong ferromagnetic (FM) interactions arising from the Mn^{3+}-O-Mn^{4+} bonds. This strong FM interaction arises from double-exchange mechanism (DE).[4] This is in addition to the superexchange interactions which are usually antiferromagnetic. In the composition range $0.2<x<0.4$, the ferromagnetism due to the DE interaction wins over the other interactions and one sees the occurrence of ferromagnetism, a metal-insulator transition, and CMR occurring at and around the ferromagnetic Curie temperature (T_c). The strong ferromagnetic interaction due to double exchange arises because both Mn^{4+} and Mn^{3+} ions have a core spin of $S=3/2$ coming from the half-filled crystal field split t_{2g} orbital and a strong intra-atomic Hund's rule coupling which spin aligns the electron in the e_g orbital which takes part in the electronic transport. The metallic state in the manganates is thus caused by ferromagnetic interactions. In addition to DE interactions the lattice distortions are believed to play an important role through strong electron-lattice coupling which arises from the Jahn-Teller distortion[5,6] around the Mn^{3+} ions. A metallic state caused by the onset of ferromagnetism is also seen in a closely related solid $La_{1-x}Sr_xCoO_3$ for $x \geqslant 0.2$. The solid has a composition driven metal-insulator transition with critical composition $x_c \approx 0.25$. In this solid the ferromagnetism and the resulting metallic behavior arises from mixed valency of Co ions (Co^{3+}/Co^{4+}) much like in the manganate.[7,8] The magnetosresistance (MR) of this solid is, however, generally small for the metallic compositions ($x \approx 0.3$), unlike the manganates.[9] Close to the critical composition range and below ($x \leqslant 0.25$), the ferromagnetic order gives way to ferromagnetic clusters. The loss of long range ferromagnetic order leads to carrier localization and to a large negative MR accompanied by memory effects and hysteresis.[9] The Co ions in this solid undergo a spin state transition (high spin/low spin), and the ferromagnetic state, onset of metallic behavior, MR, etc., depend crucially on this spin state transition. Recent transport, magnetic, and MR studies of cobaltates have established that the ferromagnetic order in this solid is of short range arising from clusters.[9,10,13] Thus cobaltates and manganates with mixed valency of the transition metal ions show a close relation between the ferromagnetic order and the metallic state. The occurrence of the metallic state is dependent on the existence of the FM interactions. However, there are important differences between the two systems. These differences arise mainly from the electronic configurations and the spin states of the transition metal ions and these lead to ferromagnetic exchange interaction of different nature. These differences also show up in the resulting ferromagnetic order which shows up below T_c.

In this paper we investigate an interesting question: What happens to the ferromagnetic order, metallic state, and the CMR when we mix a double-exchange type ferromagnet such as the manganate with a ferromagnet like the cobaltate. To study this question we have investigated the sys-

tem $La_{0.7}Ca_{0.3}Mn_{1-x}Co_xO_3$. Both the end members of the system, namely $La_{0.7}Ca_{0.3}MnO_3$ ($x=0$) and $La_{0.7}Ca_{0.3}CoO_3$ ($x=1$) are ferromagnetic. (Note that in this paper we will refer to $x=0$ as ''pure manganate'' and $x=1$ as ''pure cobaltate.'') While the composition $x=0$ shows a metallic state for $T<T_c$, the composition $x=1$ lies close to the metal-insulator transition boundary and both the compositions have low resistivity. We show that even for a small x (as low as $x\approx 0.05$) the ferromagnetic order of the pure manganate is severely modified; this leads to carrier localization and gives rise to an insulating phase. The properties of this system are governed by the nature of the electronic state of the two TM ions. Therefore, it is worth mentioning a few points regarding this aspect. The Mn ions with valency 3+ and 4+ exist in the high spin state with the electronic configuration $t_{2g}^3e_g^1$ and $t_{2g}^3e_g^0$, respectively. Both the valence states carry spin and the conduction band arises from the e_g electron which takes part in the DE interactions. The electronic configuration of the Co ions are more complicated due to the possibility of the existence of the Co ions in the low spin and the high spin states. The spin state transition occurs because the crystal field splitting and the exchange energy are comparable.[8,10] The high spin Co^{3+} ion has a configuration $t_{2g}^4e_g^2$ and the low spin ion has a configuration $t_{2g}^6e_g^0$. The low spin state is energetically more favorable. Thus trivalent Co is often found to be in a diamagnetic low spin state at room temperature and below and hence in our system we consider it to be predominantly in the low spin state. But we cannot rule out the fact that the Co ion is in a different environment when it is in the proximity of Mn ions and hence there is a finite probability of formation of high spin trivalent Co ions. The tetravalent Co ion, on the other hand, is found in the high spin state, since the high spin state with the electronic configuration $t_{2g}^3e_g^2$ is energetically lower compared to the low spin Co^{4+} ion with configuration $t_{2g}^5e_g^0$ as found by photoelectron spectroscopy.[12] The competing interactions in the system will therefore depend on the electronic state of the two TM ions in the lattice.

II. EXPERIMENTAL DETAILS

In this investigation we have carried out the following measurements in addition to chemical and structural characterization of the materials: dc magnetic susceptibility (χ_{dc}), ac susceptibility (χ_{ac}), resistivity (ρ), magnetoresistance, and the Seebeck coefficient (S). The materials were prepared by the usual solid-state reaction method. The samples with nominal composition $La_{0.7}Ca_{0.3}Mn_{1-x}Co_xO_3$ with $x=0.05$, 0.1, 0.2, 0.3, 0.5, and 1 were prepared with La_2O_3, $CaCo_3$, $MnCO_3$, and $CoC_2O_4,2H_2O$ as the starting materials. The compositions $0.05\leqslant x\leqslant 0.3$ were prepared by heating the reactants in air at 1100 °C for 32 h with intermediate grinding. The $x=0.5$ composition was prepared similarly by heating for 36 h. The $x=1.0$ composition was prepared by heating a mixture of La_2O_3, $CaCo_3$, and $CoC_2O_42H_2O$ in oxygen at 1200 °C for 24 h. Powder x-ray diffraction patterns were recorded with a RICH-SEIFERT diffractometer in the 2θ range 20° to 60°. Core level x-ray photoelectron spectra of $La_{0.7}Ca_{0.3}Mn_{0.7}Co_{0.3}O_3$ were recorded along with those of the reference compounds

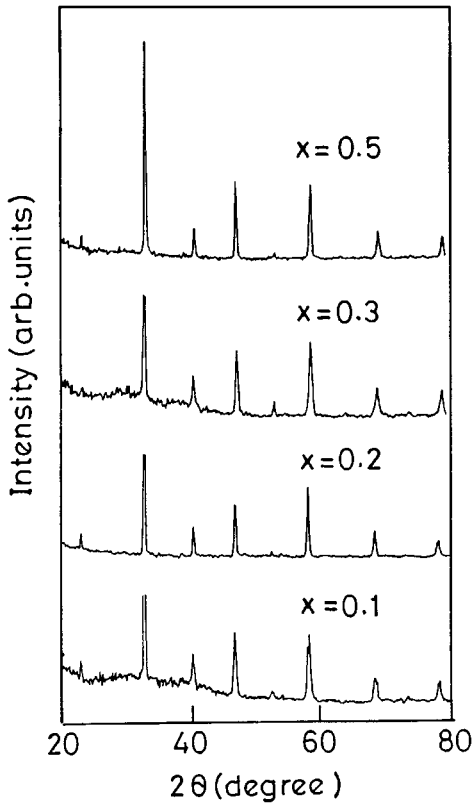

FIG. 1. Typical x-ray diffraction pattern for the $La_{0.7}Ca_{0.3}Mn_{1-x}Co_xO_3$ system.

$La_{0.7}Ca_{0.3}CoO_3$, $CaMnO_3$, $LaMnO_3$, and $LaCoO_3$ to get an idea of the oxidation states of Co and Mn. The χ_{dc} was obtained by a Faraday balance with a Lewis coil for setting up the field gradient. The typical gradient used was ≈ 55 Oe/cm. The data were taken at a maximum applied field of 0.3 T. The magnetization in the ferromagnetic state was measured both in zero-field cooled (ZFC) and field cooled (FC) states with different measuring fields ranging from 0.006 T to 0.3 T. The dc measurements were supplemented by χ_{ac} measured at 100 Hz by a standard mutual inductance bridge. The ρ were measured by a four-probe technique. While for the metallic samples ($x=0$ and $x=1$) and for $x=0.05$ the measurements were carried down to 4.2 K, for the other samples with $0.1\leqslant x\leqslant 0.5$, the ρ was measured down to 100 K because the value of ρ was large and the contact resistance becomes appreciable so that even the four-probe technique gives rise to errors. The MR was measured in fields up to 6 T using a superconducting solenoid. The Seebeck coefficient was measured using an automated standard dc technique where pure Cu forms the other arms of the thermocouple and the temperature differential was measured by a calibrated Au:Fe/chromel thermocouple.

III. RESULTS

A. Structure and the chemistry

Representative traces of the x-ray powder diffraction pattern of the system $La_{0.7}Ca_{0.3}Mn_{1-x}Co_xO_3$ are shown in Fig. 1. The end members of the series ($x=0$ and $x=1$) are cubic and have lattice parameters of 7.699 and 7.628 Å, respec-

TABLE I. Structural and magnetic parameters of the system $La_{0.7}Ca_{0.3}Mn_{1-x}Co_xO_3$. † denotes the value at the peak of the susceptibility. ‡—Below the sensitivity limit. § denotes no clear region from which the parameters can be estimated.

Composition (x)	a Å	T_c (K)	$\chi_{ac}^{\dagger}$ (cm^3/gm)	μ_{eff} (μ_B)	θ_c (K)	$M_{0.3T}$ at $T=5$ K (emu/gm)
0	7.699	260	0.060	5.80	260	84
0.05	7.733	190	0.012	5.63	225	
0.1	7.726	170	0.0105	5.45	215	
0.2	7.718	165	0.009	5.25	215	
0.3	7.695	165	0.0007	4.97	180	15
0.5	7.664	165	‡	§	§	
1.0	7.628	160		3.48	240	26

tively. The samples $0.05 \leqslant x \leqslant 0.5$ could be indexed on the basis of a pseudocubic unit cell; the pseudocubic lattice parameters calculated using the least square refinement technique are given in Table I. On substitution of Mn by Co the structure does not undergo any change, but there is a systematic decrease in the lattice parameter as the Co content increases. The decrease in the lattice constant can be related to the smaller ionic radii of the Co ion. From the core level x-ray photoelectron spectra, we are able to qualitatively determine the oxidation states of Co and Mn. The Mn($2p$) binding energy of $La_{0.7}Ca_{0.3}Mn_{0.7}Co_{0.3}O_3$ was found to be 624 eV, which is between the binding energies of Mn^{3+} and Mn^{4+}, suggesting the presence of both the oxidation states. The Co($2p$) spectrum gave a Co($2p$) binding energy of 781 eV and is similarly interpreted to be a mixture of both Co^{3+} and Co^{4+}. There was no evidence for the presence of Co^{2+}.

B. Magnetic properties

In Fig. 2 we show the χ_{ac} as a function of T for all the $La_{0.7}Ca_{0.3}Mn_{0.7}Co_{0.3}O_3$ samples measured. Table I shows the important parameters obtained from the magnetic measurements. Similar values of T_c have been obtained from both χ_{ac} and magnetization measurements. T_c as well as the magnitude of χ_{ac} are suppressed severely in the mixed systems. In Fig. 3 we show the χ_{dc} measured in the paramagnetic phase for the different samples. The data are plotted as χ_{dc}^{-1} vs T. We find that the Curie-Weiss law is followed at least in a limited temperature range above T_c over which the data are taken, barring the sample $x=0.5$ which clearly shows two regions with different values of the Curie constants and the paramagnetic Curie temperatures. The effective moments μ_{eff} obtained from the Curie constants are also shown in Table I, along with the paramagnetic Curie temperatures, θ_c. The values of the μ_{eff} show a gradual decrease on Co substitution. θ_c also is reduced as x is increased, showing a general weakening of the ferromagnetic DE interaction and an increasing contribution of AFM interactions arising from superexchange. For the end members $T_c \approx \theta_c$; however, for other compositions there is significant difference between the two. The peak values of the ac susceptibilities (χ_{ac}) are less in the mixed systems (see Fig. 2) and it is the least for the compositions $x=0.3$. (Note that the χ_{ac} could not be measured for the $x=0.5$ sample since the signal was very small.) This lowering of the peak value of χ_{ac} most

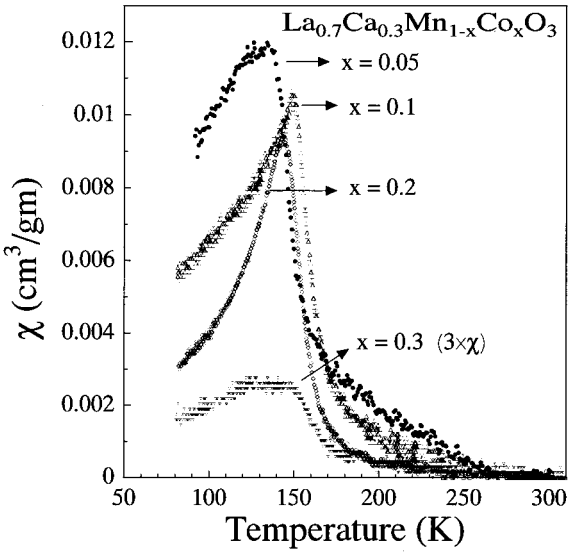

FIG. 2. ac susceptibility (χ_{ac}) measured at 100 Hz.

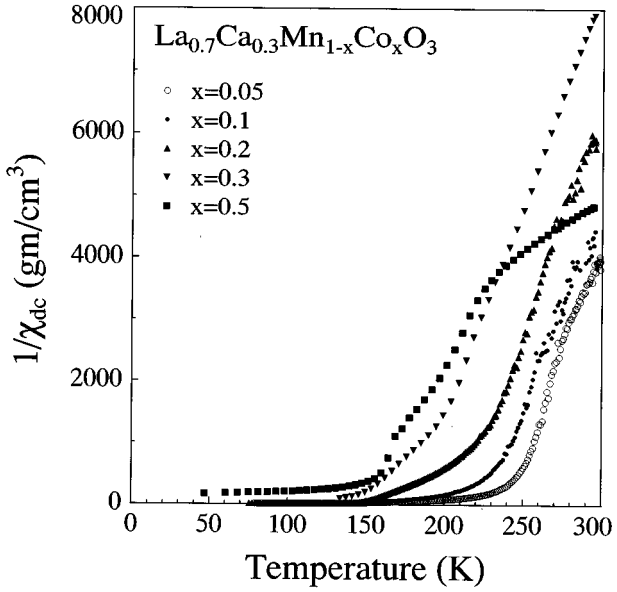

FIG. 3. Curie-Weiss plot of the dc susceptibility (χ_{dc}).

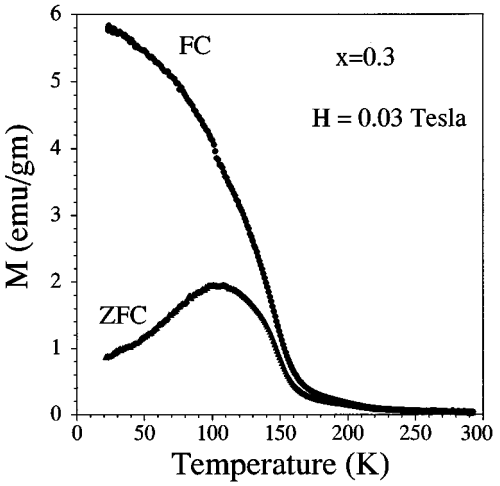

FIG. 4. Field cooled and zero-field cooled magnetization measured in a field of $H_{meas}=0.03$ T for the sample $x=0.3$.

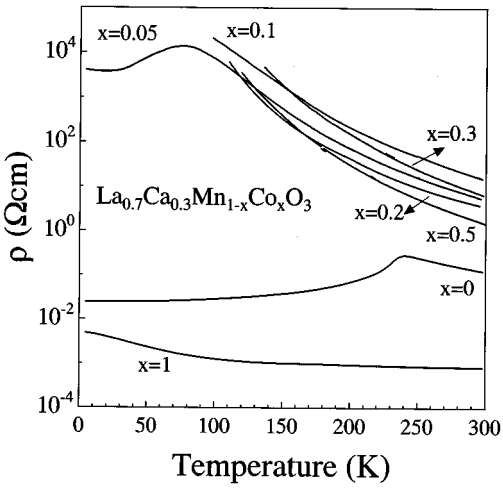

FIG. 5. Resistivity as a function of temperature.

likely arises from the decrease in the magnetization (M_{dc}), which decreases on Co substitution. The onset of the mixed type ferromagnetic exchange interactions on Co substitution, therefore, weakens the ferromagnetic order as well as lowers the magnetic moment. One interesting observation is the behavior of the temperature dependence of χ_{ac} below T_c. For the pure manganate ($x=0$), χ_{ac} is nearly constant below T_c.[14] But for the pure cobaltate ($x=1$) the χ_{ac} decreases sharply as T is lowered.[9] A similar behavior is seen for the mixed systems. Even a small amount of Co substitution renders the temperature dependence of χ_{ac} below T_c similar to that in the pure cobaltate. The absence of a proper long range FM order can be seen in the temperature dependences of the FC and the ZFC magnetizations. This can be seen as an example for the sample $x=0.3$ in Fig 4. The FC and ZFC magnetizations are denoted as M_{FC} and M_{ZFC}, respectively. The drop of the M_{ZFC} below 100 K deserves attention. In the pure manganate which shows proper long range order, M_{ZFC} for $T<T_c$ is almost independent of T. In contrast, M_{ZFC} of the cobaltate decreases appreciably on cooling below T_c. From previous magnetic studies as well as the neutron studies it has been proposed that the ferromagnetic state seen in the cobaltate is of a cluster glass type.[13] The drop of the M_{ZFC} for $T<T_c$ has been interpreted as a signature of this cluster glass behavior. A similar behavior of the M_{ZFC} is also seen in the mixed system. The magnetic behavior of the mixed systems being similar to that of the cobaltates, one may infer that the long range order of the pure manganates gives way to cluster glass. We will discuss the implications of these observations below.

C. Resistivity and magnetoresistance

In Fig. 5 we show the temperature dependence of ρ. It can be seen that both end members have a very low ρ. Over the entire temperature range the pure cobaltate ($x=1$) has a resistivity, $\rho<10$ m Ω cm and the pure manganate (x=0) has a resistivity $\rho<100$ m Ω cm. For the mixed systems the ρ are very high and at $T=100$ K $\rho>10^4$ Ω cm. The pure cobaltate is at the boundary of the metal-insulator transition. It has a shallow temperature dependence of ρ for $T>100$ K and ρ rises slightly below 100 K due to the spin state transition of the Co ions.[9,10] The hole doped manganates (with no Co substitution) show a transition to the metallic state below T_c when the hole doping is in excess of 0.2 per formula unit. But for the mixed system we find an insulating behavior over the entire temperature range (down to 100 K) except for the sample with $x=0.05$. The resistivity of the $x=0.05$ sample is also very high but it shows a shallow peak in ρ at $T\ll T_c$. We thus see a charge localization and destruction of the metallic behavior on Co substitution. The carriers are localized over the entire composition range ($0.1\leqslant x\leqslant 0.5$) although we have the presence of strong ferromagnetic exchange and ferromagnetic order, albeit of cluster type. The shallow peak in ρ at low temperatures in the $x=0.05$ sample can be explained as follows. For this composition the material can be considered as a ''composite'' containing metallic and insulating regions. The metallic regions are mostly of composition close to $x=0$ sample. This is a result of the chemical inhomogeneity in these materials in a microscopic scale. As T is reduced the ρ of the metallic regions decrease while that of the insulating regions increase. This leads to increasing current paths through the metallic regions of low resistivity. Ultimately the conduction from the metallic regions predominates and ρ decreases as T is reduced. The shallow peak in ρ thus signifies a crossover. For $x\geqslant 0.05$ the metallic regions make marginal contribution to conductivity even if they are present in small volume fractions.

The MR as a function of temperature (measured with a field $H=6$ T) is shown in Fig. 6. The MR is defined as

$$\frac{\Delta\rho}{\rho}=\frac{\rho[H]-\rho[H=0]}{\rho[H=0]}. \tag{1}$$

$\rho[H]$ is the value of ρ in an applied field of H. The MR is negative for all the samples. But the CMR of the manganate ($x=0$) is suppressed even with small Co substitution. The magnitude of the MR (measured at $H=6$ T) shows a monotonic decrease as x increases. For $x=0.1$ it is 80% at 100 K and this decreases to nearly 2% for $x=0.5$. For the two end members the nature of the MR is somewhat different. For the pure manganate ($x=0$) the value of the MR is highest near

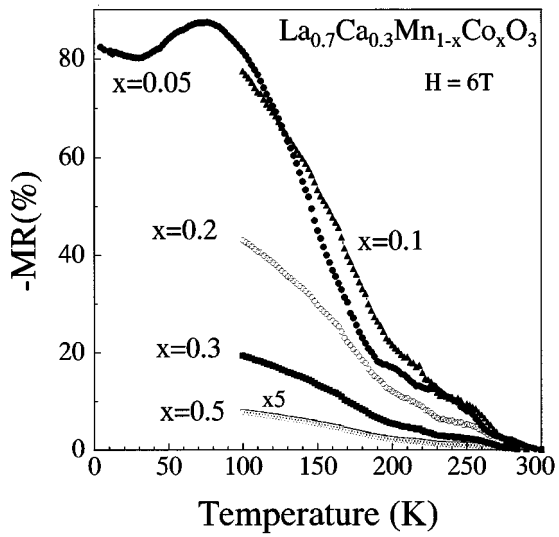

FIG. 6. MR as a function of temperature measured at a field $H=6$ T.

the transition. For the pure cobaltate ($x=1$) the MR is negative but much smaller and is appreciable also near the T_c.[9] In contrast, the MR in the mixed system monotonically decreases as T increases and becomes very small close to T_c. The MR close to T_c shows a series of small features in almost all the samples. This is more perceptible in the samples with lower Co content. To magnify these features we plot in Fig. 7 the logarithmic derivative $d\ln\mathrm{MR}/dT$ as a function of T. In the same graph for comparison we show in the inset the logarithmic derivative $d\ln\chi_{\mathrm{dc}}/dT$. The derivative curves for the χ_{dc} show a number of features which closely follow similar features in the MR curve. Interestingly, the features occur in all the compositions at similar temperatures. A plateau or a small peaklike feature in the MR curve will be seen as a peak in this derivative curve.

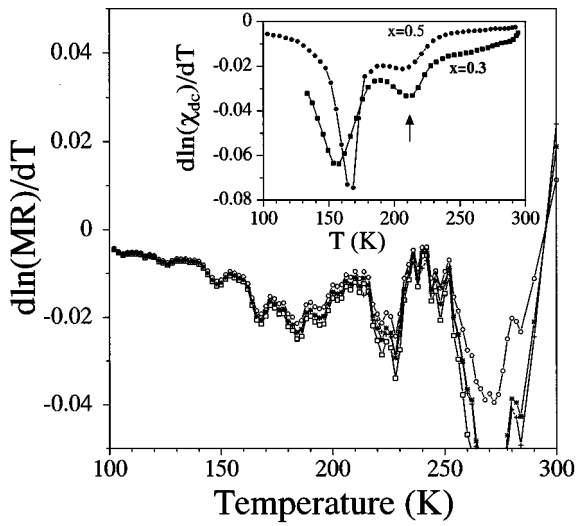

FIG. 7. The logarithmic temperature derivative of the magnetoresistance $d\ln(\mathrm{MR})/dT$ as a function of T for different samples. The inset shows the derivative $d\ln\chi_{\mathrm{dc}}/dT$ for the samples $x=0.3$ and $x=0.5$.

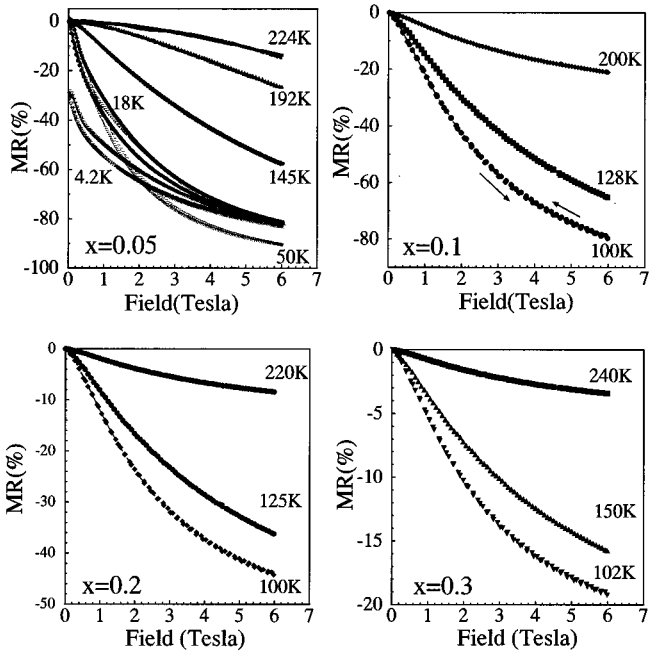

FIG. 8. MR as a function of field H at different temperatures for different samples. For the $x=0.05$ sample the MR at $T=4.2$ K shows a strong memory effect, hysteresis, and nonclosure of the resistivity value on field cycling.

(The derivative curve for the MR will have an overall negative sign because the MR decreases as the T increases.) The most prominent of the features occur near the 240–250 K region, which is also the region where the end member ($x=0$) has its T_c. The $d\ln\chi_{\mathrm{dc}}/dT$ curve shows the smaller feature in this region (marked by arrow in the inset of Fig. 7). There are 3–4 such peaklike features in the MR curve persisting down to 150 K. This multitude of peaks can arise from the ferromagnetic clusters formed near the T_c which eventually freeze for $T<T_c$. For $T\ll T_c$, the derivative curve is more or less featureless, showing that the MR decreases smoothly as T increases. The field dependences of the MR (see Fig. 8) seen in the mixed systems are also different from those seen in the pure manganates. In the pure manganate the field dependence has two distinct regions.[14] In the low field region ($H<1$ T) the MR rises almost linearly in H. This is followed by a second region where the MR exhibits a slow dependence on the applied field showing an approach to saturation. By contrast, the MR in the mixed system does not show a clear separation of the two regions; also there is no clear sign of the saturation in MR in the high field. The MR seems to approach the saturation (if any) asymptotically. This is similar to the behavior in the cobaltates, where in a certain composition range close to the critical range, the MR shows a linear (or almost linear) dependence on H for H up to 6 T.[9] This absence of saturation is also seen in the magnetization measurements, implying that even at our highest fields accessible the spins have not aligned completely to the field direction.[10,13] This suggests that we might have clusters of spins aligned ferromagnetically interspersed by regions where the spins do not belong to a ferromagnetic cluster and retain their random orientations which may be blocked by a local anisotropy field. The field dependence of

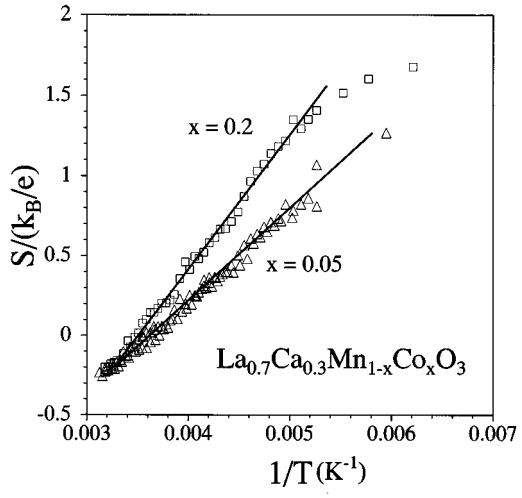

FIG. 9. The Seebeck coefficient (S) as a function of $1/T$ for two samples $x=0.05$ and $x=0.2$. S has been scaled by k_B/e. The lines are fit to the data as described in the text.

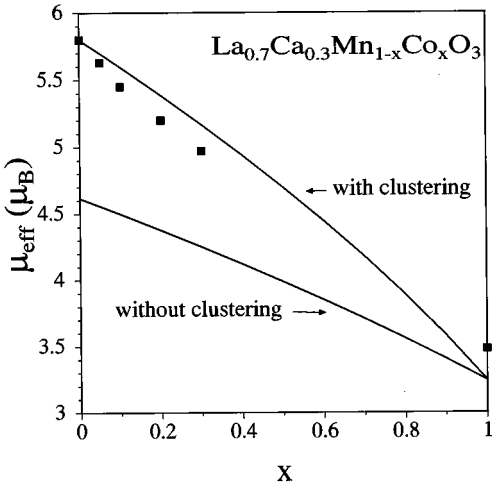

FIG. 10. The effective magnetic moment (μ_{eff}) as a function of x. The calculated curves were obtained on the assumption that all Co^{3+} are in the low spin state and all Co^{4+} are in the high spin state. The two calculated curves are explained in the text.

MR and the magnetization behavior of the mixed systems are very similar to those of the cobaltates even for small x. In the cobaltates, in the critical region where the magnetic behavior is determined by the dynamics of cluster freezing, the MR shows strong hysteresis.[9] In the mixed systems (except $x=0.05$) despite the fact that the ferromagnetic state seems to be dominated by clusters, we do not see any hysteresis behavior down to 100 K. For the $x=0.05$ sample we see the hysteresis only at $T=4.2$ K. Since we could not do MR measurements for the other compositions below 100 K, we cannot rule out these effects at lower temperatures.

D. Seebeck coefficient

The measured Seebeck coefficients (S) for the mixed system show a $1/T$ dependence, as expected in solids with localized carriers. This is shown in Fig. 9 for two samples $x=0.05$ and $x=0.2$. S has been scaled by $k_B/e = 86$ μV/K. The data are somewhat noisy due to the high sample resistances. The S of the mixed systems are clearly different from those of the two end members.[10,11] We see a deviation from the $1/T$ dependence at $T<T_c$. Other than that no special features are seen near T_c unlike the hole doped manganates with no Co substitution.

IV. DISCUSSION

In this section we discuss some of the important observations made in the present investigation and their implications. The focus of our discussion is the question as to what happens to the ferromagnetic metallic state arising from the DE interaction when it is mixed with other type of ferromagnetic interactions. All the present data have shown that the ferromagnetic order and the metallic state arising from the DE interaction are ''fragile.'' Even a small amount of Co ions seems to destroy the long range ferromagnetic order, the metallic state, and most importantly, the CMR. In the following we discuss some of the important effects of Co substitution.

A. Susceptibility above T_c

It has been pointed out before that, at least in a limited temperature range available in this measurement, the susceptibility above T_c follows Curie-Weiss law (except for the sample $x=0.5$). The μ_{eff} are given in Table I. In Fig. 10 we have plotted μ_{eff} as a function of x. It can be seen that μ_{eff} decreases continuously as x increases and this arises because on Co substitution we are decreasing the density of moment-carrying Mn ions and most of the Co^{3+} ions are in $S=0$ low spin configuration ($t_{2g}^6 e_g^0$). As a check we have plotted in Fig. 10 the calculated μ_{eff} as a function of x with values of moments equal to the spin-only values and with the assumption that all the Co^{3+} are in the low spin state and all the Co^{4+} are in the high spin state ($t_{2g}^3 e_g^2$). (Note: The assumption that all Co^{3+} are in the low spin state may not be entirely correct. But, considering the fact that we do not have any independent measure for the population of the high spin and low spin states, we have to make this plausible assumption.) The calculated curve shows the correct trend of the data but lies systematically below the data points. In fact, the deviation starts from the pure manganates ($x=0$) and the trend persists over the entire composition range studied. In case of manganates, as has been discussed in Ref. 15, there is a local clustering of Mn^{3+} ions around a Mn^{4+} ion due to strong ferromagnetic interactions. We account for this clustering by taking the S_{eff} which is higher than their spin-only values of both Mn^{3+} and Mn^{4+} ions. We can make the calculated μ_{eff} for the $x=0$ sample agree with the observed μ_{eff} by taking $S_{\text{eff}} = 2.45$. We show in Fig. 10 also the curve calculated with the new value of effective spin ($S_{\text{eff}} = 2.45$) for the Mn ions (marked as ''with clustering''). The agreement with the observed data is better, indicating that a similar type of local clustering of spins of the Mn ions persist even in the Co substituted samples.

B. The magnetic order

In the pure manganate ($x=0$) the local clustering of the Mn^{3+} ions around a Mn^{4+} eventually leads to a ferromag-

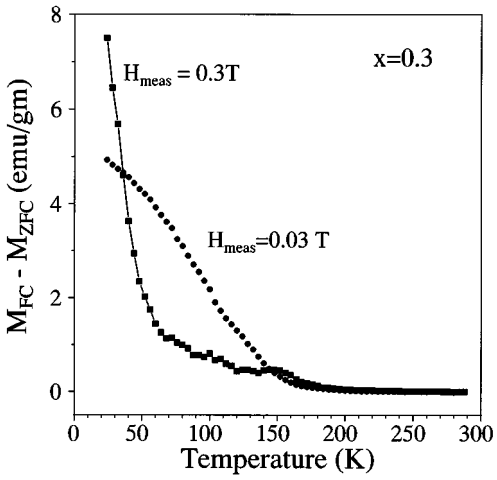

FIG. 11. The difference ($M_{\mathrm{FC}}-M_{\mathrm{ZFC}}$) as a function of T for two different measuring fields (H_{meas}).

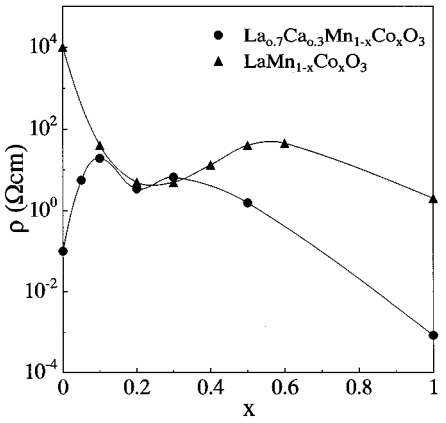

FIG. 12. The room temperature resistivities of the two systems, $La_{0.7}Ca_{0.3}Mn_{1-x}Co_xO_3$ and $LaMn_{1-x}Co_xO_3$ (data from Ref. 16) as a function of x.

netic order of the long range type. The lack of proper ferromagnetic long range order in the pure cobaltates ($x=1$) arises due to the same reason that the diamagnetic low spin Co^{3+} ions dilute the magnetic lattice.[10] In the $x=0$ sample, the calculated saturation moment (n_s) assuming complete spin alignment is $\approx 3.7\mu_B$/Mn ion and this is close to the experimentally observed n_s. On the other hand, in pure cobaltate ($x=1$), the observed $n_s \approx 1.4\mu_B$/Co ion is less than the expected value of $1.8\mu_B$. (The n_s has been obtained at 6 T and 4.2 K.) Also, as mentioned earlier the M-H curve does not show full saturation of the magnetic moment even for an applied field of 6 T. This particular feature is even more prominent in the mixed samples. For instance in the sample $x=0.3$, the observed n_s at 6 T and 4.2 K is only $0.8\mu_B$ and the calculated moment for full spin alignment is $\approx 3.8\mu_B$. This indicates that we do not have complete spin ordering below T_c. A likely scenario is that the existence of mixed exchange (i.e., presence of both ferromagnetic as well as antiferromagnetic exchange), as well as dilution by the diamagnetic low spin Co^{3+} ions, lead to disorder or canting of spins preventing complete ferromagnetic spin alignments. It is also possible that we have ferromagnetic clusters of finite dimensions which order below a certain temperature, albeit randomly, due to random anisotropy. The resulting magnetic order below T_c therefore can be looked upon as a diluted ferromagnet created by the mixed exchange. The multiple peaklike structures in the $d\ln\chi_{\mathrm{dc}}/dT$ curve shown in the inset of Fig. 7 carries signatures of these clusters freezing over a range of temperatures around T_c.

The absence of a proper long range order is also seen from the difference in the FC and ZFC magnetizations. This difference becomes large below a certain temperature, depending on the measurement field (H_{meas}). In Fig. 11 we plot $\Delta M = M_{\mathrm{FC}} - M_{\mathrm{ZFC}}$ as a function of T as measured in two different fields (0.03 T and 0.3 T). ΔM measured at a certain field (H_{meas}) arises when $H_{\mathrm{meas}} < (H_a)$, where H_a is a local anisotropy field which locks the spin in certain orientation depending on the direction of the local field. For good ferromagnets the ΔM should be small and essentially temperature independent. For $H_a < H_{\mathrm{meas}}$, $\Delta M \approx 0$. However, if H_a increases rapidly as T is decreased, ΔM will also rise as T is lowered. The rapid rise of ΔM starts at the temperature when the H_a becomes larger than H_{meas} on cooling. This rapid rise of ΔM will happen at lower temperatures for higher H_{meas} because the crossover condition $H_{\mathrm{meas}} \approx H_a$ will happen at lower T. The temperature dependence of ΔM seen in Fig. 11 thus can be explained as due to existence of a local anisotropy field which becomes large as T is reduced. This can give rise to the observed cluster glass type behavior. We see this behavior in all the mixed samples as well as in the pure cobaltate ($x=1$). To summarize, we find that the Co substitution breaks down the long range ferromagnetic order seen in the pure manganates, replacing it with cluster type of ferromagnetic order. This breakdown of ferromagnetic order can arise both from the mixed exchange as well as the dilution by low spin diamagnetic Co^{3+} ions.

C. Comparison with $LaMn_{1-x}Co_xO_3$

The system under investigation, $La_{0.7}Ca_{0.3}Mn_{1-x}Co_xO_3$, has a close relationship with the system $LaMn_{1-x}Co_xO_3$ which has no Mn^{4+} ions arising from the Ca substitution. Structurally, both systems are similar. Within the composition range $0.15 < x < 0.5$, the system $LaMn_{1-x}Co_xO_3$ has a pseudocubic structure.[16] For $x < 0.15$ it has an orthorhombic structure. In our system, over the entire composition range we find a pseudocubic structure. In addition to the structure, there is a striking similarity in the room temperature resistivities of the two systems for an intermediate range of x as shown in Fig. 12. (Data for the $LaMn_{1-x}Co_xO_3$ system are taken from Ref. 16.) There is a striking similarity between the two systems especially for $0.1 \leqslant x \leqslant 0.4$. (Note that the data for $x=0.5$ from the Ref. 16 may not be reliable because this sample was not single phase.) It seems that in this composition range the presence of the Mn^{4+} ions does not make much difference. In the system without Ca, the resistivity decreases sharply on Co substitution, though it still remains insulating. The decrease in the resistivity over the narrow composition range $0 < x < 0.15$ was attributed to the removal of Jahn-Teller distortion on Co substitution.[16] In our system, the influence of Ca is apparent only very close to the end members, and as the Co content increases the resistivities increase drastically. This sudden increase in resistivity even

for the $x=0.05$ sample cannot be explained by considering only dilution effect arising from the diamagnetic Co ions. It is a well-known fact that substitution of the divalent ions for La in the pure $LaMnO_3$ and hence the formation of tetravalent Mn ions, removes the lattice distortion; hence the resistivity decreases.[17] When Co is substituted for the Mn ions the amount of Mn^{4+} in the system decreases and it is likely that a certain amount of lattice distortion arises again. This increases the resistivity and makes the ρ of both systems comparable. There is an added effect of the low spin diamagnetic Co^{3+} ion in the system, which essentially decreases the pathways for the hopping. We discuss the issue of the effect of the lattice distortion more quantitatively in the next subsection.

D. Charge localization

In the solid under investigation, $La_{0.7}Ca_{0.3}Mn_{1-x}Co_xO_3$, both the end members being metallic, the most important observation is the charge localization over almost the entire composition range studied ($0.05 \leqslant x \leqslant 0.5$). The charge localization leads to a temperature dependence of ρ which can be described by two distinct approaches. First is the variable range hopping in a Coulomb gap (VRH) (Ref. 18) and the second is charge localization due to lattice distortion (polaron formation).[20] We discuss both of the mechanisms below. We find that our data can be fitted to the VRH equation,[18]

$$\rho=\rho_0 \exp[\sqrt{T_0/T}], \tag{2}$$

to a reasonably good degree. (Note that the VRH equation of the Mott type, i.e., with the exponent 1/4 does not give a good fit to the data.) The characteristic temperature represented by T_0 is large and $T_0 \approx (7-10)\times 10^4$ K. Since $T_0 \propto 1/\langle \xi \rangle$, where $\langle \xi \rangle$ is the average localization length, this would imply that the charge is localized in a small length scale. An estimate of the localization length from T_0 shows that $\langle \xi \rangle \approx$ 2.5–5 Å, which is of the order of the unit cell dimension. This is a reasonable order for $\langle \xi \rangle$. The values of the prefactor ρ_0 are in the range 3–50 $\mu\ \Omega$ cm. This value of ρ_0 is unphysical. Typical ρ_0 should be of the order of $\approx \rho_{\mathrm{mott}}$, the maximum metallic resistivity.[19] ρ_{mott} for these oxides are seldom below 1–10 m Ω cm.[8] This makes the VRH an unreasonable proposition even if the data fit to Eq. (2) quite well.

We next examine the other possibility. Recently, there is increasing evidence that the T dependence of ρ can be described using the concept of small polarons which can arise from the strong lattice-electron interaction originating from the Jahn-Teller distortion.[21,22] The small polaron size is typically of the order of one unit cell. For $T > \theta_D/2$ (θ_D is the Debye temperature) the carrier transport is by thermal activation; the resistivity is given by the equation:[21,22]

$$\rho=\left[\frac{\hbar a}{e^2}\right]\left[\frac{T}{T_p}\right]^n\left[\frac{1}{c(1-c)}\right]\exp\left(\frac{E+W-\lambda^{3-2n}}{k_BT}\right), \tag{3}$$

where a is the hopping distance which we take as approximately the Mn-O-Mn distance ($\approx$ 3.8 Å). c is the polaron concentration, $2W$ is the polaron formation energy, k_BT_p is a characteristic polaron energy scale which gives the polaron tunneling rate,[20] λ is the transfer integral, and E is the energy required to produce intrinsic carriers. For $k_BT_p \gg \hbar\omega_p$ (ω_p is the characteristic phonon frequency involved in polaron formation), the transport is adiabatic[20] and the exponent $n=1$ in Eq. (3). In the other extreme, for nonadiabatic transport $n=1.5$. The Seebeck coefficient (S) for this polaronic transport process is given by[21,22]

$$\frac{S}{(k_B/e)}=\left[\frac{E}{k_BT}-\ln\left(\frac{5}{4}\right)-\ln\frac{c(1-c)}{(1-2c)^2}\right]. \tag{4}$$

From the data on S we find that Eq. (4) holds good for $T > T_c$. For $x=0.05$ sample we find $E=47$ meV and $c=0.40$. For the $x=0.2$ sample we get $E=69$ meV and $c=0.41$. Thus on increasing x the activation energy E increases while c stays close to 0.4. The expected $c \approx 0.3$. This indicates a slight oxygen excess. The corresponding value of E for the pure manganate is much lower (typically 10–20 meV).[14,21] (However, there is an element of uncertainty in the determination of E from the thermopower data for the pure manganates because the thermopower near T_c, in particular the peak is S, is very sensitive to the exact Mn^{4+} content[11] and one may obtain different values for E depending on how far one is from the peak in S. But the values of E for this composition range lie in the range stated before.) According to Eq. (4), S has the form $S=A/T+B$. A/T is always positive and for $c \approx 0.3$–0.4 B is negative. The resulting sign of S at a given T will be determined by the relative strengths of these two terms. In the Co substituted system the activation energy E being large the A/T term dominates over most of the temperature range leading to a positive S. However, for the unsubstituted system ($x=0$) E being small, S can be negative for $T > T_c$ since the B term (which is negative) will have a larger magnitude. This explains the positive sign of S in the more localized Co substituted systems.

The resistivity data can be fitted to Eq. (3) equally well for both $n=1$ or 1.5. As a result from the fit alone it is difficult to decide if the polaron hopping is adiabatic ($n=1$) or nonadiabatic ($n=1.5$). For the pure manganate ($x=0$) the value of k_BT_p is relatively large and for this sample the polaron transport may be nearly adiabatic so that from the fit [using $n=1$ in Eq. (3)] we obtain $(E+W-\lambda) \approx 122$ meV and $T_p \approx 200$ K. For the mixed samples the T_p being small (typically $\leqslant 100$ K) the transport is nonadiabatic. From the fit to Eq. (3) using $n=1.5$, we obtain $(E+W) \approx 135$–160 meV for all the samples. As an example, for the sample $x=0.2$ we find $(E+W)=160$ meV and $T_p = 55$ K. Using $E \approx 69$ meV, obtained from the S data, we find $W \approx 91$ meV. For nonadiabatic transport T_p, λ, and W are related by[21] $k_BT_p=(\pi\lambda^4/4W)^{1/3}$. From this relation we obtain the value of the transfer integral $\lambda \approx 11$ meV. This value of λ is of the correct order. We thus find that the resistivity and the Seebeck coefficient can be reasonably explained from the view of polaronic transport. The Co substitution increases the activation energy E. Therefore it seems that the strong carrier localization in the mixed system most likely has its origin in the lattice distortion and the resulting polaron formation, and the increase in the resistivity on substitution of even a small amount of Co may most likely be due to the onset of lattice distortion, since the Mn^{4+} is being decreased when Co is substituted.

V. CONCLUSION

We have made a systematic investigation of the effect of dilution of Mn by Co on the electrical and magnetic properties of the GMR system $La_{0.7}Ca_{0.3}MnO_3$. The magnetic measurements point towards the breakdown of the long range ferromagnetism (as seen in the parent Mn compound) on substitution of even a small amount of Co (as small as $x \approx 0.05$). The type of magnetism formed in the substituted compound can be related to the cluster glass type (as seen in the system closely related to the other end member of the series, $La_{0.7}Sr_{0.3}CoO_3$). The influence on the resistivity is even more drastic as the resistivity increases by orders of magnitude (nearly 3–4 orders) compared to the end members. The highly insulating behavior could be explained as due to polaronic lattice distortion. Since the long range ferromagnetic order is weakened by the Co, the magnetoresistance is also affected and the MR decreases as the Co content increases in the system. Thus we can conclude that the double exchange and the resulting metallic state as seen in the CMR oxides is very ''fragile'' and even a small amount of Co alters the magnetism, the metallic state, and also the magnetoresistance properties of the CMR oxide.

ACKNOWLEDGMENTS

One of us (A.K.R.) wants to thank the Department of Science and Technology, Government of India for a sponsored scheme. N.G. wants to thank Council of Scientific and Industrial Research for support. The help of Ayan Guha during the preparation of the manuscript is acknowledged.

*Electronic address: gayathri@physics.iisc.ernet.in
†Electronic address: arup@physics.iisc.ernet.in

[1] G. H. Jonker and J. H. Van Santen, Physica (Amsterdam) **16**, 337 (1950).
[2] K. Chanara *et al.*, Appl. Phys. Lett. **63**, 1990 (1993).
[3] R. von Helmolt, J. Wecker, B. Holzapfel, L. Schwltz, and K. Samwer, Phys. Rev. Lett. **71**, 2331 (1994).
[4] C. Zener, Phys. Rev. **82**, 403 (1951); P. G. deGennes, *ibid.* **118**, 141 (1960).
[5] J. B. Goodenough, Phys. Rev. **100**, 564 (1955).
[6] A. J. Millis, P. B. Littlewood, and B. J. Shraiman, Phys. Rev. Lett. **74**, 5144 (1995).
[7] G. H. Jonker and J. H. Van Santen, Physica (Amsterdam) **19**, 120 (1953).
[8] P. Ganguly and C. N. R. Rao, in *Metallic and Non-metallic State of Matter*, edited by P. P. Edwards and C. N. R. Rao (Taylor and Francis, London, 1985).
[9] R. Mahendiran and A. K. Raychaudhuri, Phys. Rev. B **54**, 16 044 (1996).
[10] M. A. Senaris-Rodriguez and J. B. Goodenough, J. Solid State Chem. **118**, 323 (1995).
[11] R. Mahendiran, S. K. Tiwary, A. K. Raychaudhuri, R. Mahesh, and C. N. R. Rao, Phys. Rev. B **54**, R9604 (1996).
[12] A. Chainani, M. Mathew, and D. D. Sarma, Phys. Rev. B **46**, 9976 (1992).
[13] M. Itoh, I. Natori, S. Kubota, and K. Motya, J. Phys. Soc. Jpn. **63**, 1486 (1994).
[14] R. Mahendiran, S. K. Tiwary, A. K. Raychaudhuri, T. V. Ramakrishnan, R. Mahesh, N. Rangavittal, and C. N. R. Rao, Phys. Rev. B **53**, 3348 (1996).
[15] J. Tanaka, H. Nozaki, S. Horiuchet, and M. Tsukioka, J. Phys. (France) Lett. **44**, L129 (1983).
[16] G. H. Jonker, J. Appl. Phys. **37**, 1424 (1966).
[17] J. B. Goodenough, Prog. Solid State Chem. **5**, 145 (1971).
[18] B. I. Sholvskii and A. L. Efros, *Electronic Properties of Doped Semiconductors* (Springer, Berlin, 1984).
[19] N. F. Mott and E. A. Davis, *Electronic Processes in Noncrystalline Materials* (Clarendon Press, Oxford, 1971).
[20] D. Emin, Adv. Phys. **24**, 305 (1975).
[21] M. Jaime, M. B. Salamon, M. Rubinstein, R. E. Treece, J. S. Horwitz, and D. B. Chrisey, Phys. Rev. B **54**, 11 914 (1996).
[22] R. Raffaelle, H. V. Anderson, D. M. Sparlin, and P. E. Parris, Phys. Rev. B **43**, 7991 (1991).